Belén Cabal, Félix Quintero, Luís Antonio Díaz, Fernando Rojo, Oliver Dieste, Juan Pou, Ramón Torrecillas and José Serafín Moya, " Nanocomposite of silver nanoparticles embedded in glass nanofibres obtained by laser spinning ", Nanoscale, **5**, 3948-3953, 2013.

https://doi.org/10.1039/C3NR00638G

Journal Name

Dynamic Article Links ►

Cite this: DOI: 10.1039/c0xx00000x

www.rsc.org/xxxxxx

ARTICLE TYPE

Nanocomposite of silver nanoparticles embedded in glass nanofibres obtained by laser spinning

Belén Cabal*[a], Félix Quintero[b], Luís Antonio Díaz[a], Fernando Rojo[c], Oliver Dieste[b], Juan Pou[b], Ramón Torrecillas[a] and José Serafín Moya[d]

Received (in XXX, XXX) Xth XXXXXXXXX 20XX, Accepted Xth XXXXXXXXX 20XX
DOI: 10.1039/b000000x

A nanocomposite made of non-woven glass fibres with diameters ranging from tens of nanometers up to several micrometers, containing silver nanoparticles were successfully fabricated by laser spinning technique. Pellets of a soda-lime silicate glass containing silver nanoparticles with varying concentration (5 and 10 wt.%) were used as a precursor. The followed process to obtain the silver nanofibres did not agglomerate significantly the metallic nanoparticles, the average particles size is still lower than 50 nm. This is the first time that glass nanofibres containing silver nanoparticles were obtained following a process different from electrospinning of a sol-gel, thus avoiding the limitations of this method and opening up a new route to composite nanomaterials. Antibacterial efficiency of the nanosilver glass fibres, tested against one of the most common Gram negative bacteria, was greater than 99.99 % compared to the glass fibres free of silver. The silver nanoparticles are well-dispersed not only on the surface but also embedded into the uniform nanofibres, which leads to a long lasting durable antimicrobial effect. All these novel characteristics will potentially open up a whole new range of applications.

Introduction

Organic and inorganic nanofibres functionalized with metal nanoparticles are promising materials for numerous applications in catalysis, environmental science and energy and biomedical technology.[1-3] Recent works developed processes for the production of different combinations of this kind of nanocomposites. Some examples are the deposition of Au nanoparticles on titania nanofibres for catalysis;[4] anatase nanofibres with Pt nanoparticles for the construction of fuel cell membranes;[5] and Au nanoparticles on ZnO nanofibres for sensing.[6] In particular, silver nanoparticles demonstrated high performance for catalysis and antibacterial applications. For these reasons, numerous efforts are being directed to the development of fibrous nanocomposites with silver nanoparticles. For instance, the greatest advances in water purification in recent times are associated with silver technology.[7] Specifically, Nangmenyi et al. demonstrated high performance for water filtering and disinfection applications by impregnating with Ag nanoparticles commercially available E-glass fibres with diameters in the range of several micrometers.[8-10]

Silver nanoparticles can be incorporated into the bulk of polymer nanofibres by adding a metal salt to the precursor sol-gel and reducing it before electrospinning.[11] Conversely, the silver nanoparticles can be dispersed on the surface of the polymeric nanofibre by addition of the metal salt to the polymer solution and reduction[12] or by ion exchange with the nanofibres in aqueous solution after electrospinning.[13, 14] In all these methods the nanofibres are formed by electrospinning of a polymer precursor. Consequently, limited compatibility of polymers with some metal salts, make it difficult to develop new types of spinnable sol-gel solutions.[1]

In order to take advantage of the higher thermal, mechanical and chemical resistance of ceramic nanofibres, some researchers developed new nanocomposites composed of silica nanofibres containing silver nanoparticle for catalytic and medical applications. All these works rely on electrospinning combined with different routes for the addition of metal nanoparticles to the fibres. In some cases,[15-17] the silver is added as $AgNO_3$ to the precursor sol-gel before spinning and the calcination process of the fibres at temperatures exceeding 400ºC renders the silica nanofibres with the silver nanoparticles obtained by thermal reduction. An alternative method relies on the addition of the silver nanoparticles to the silica nanofibres by incubating the fibres in aqueous solution of silver nitrate.[18] These methods must deal with the problems of agglomeration of metal nanoparticles during formation and their uniform distribution. On the other hand, the glass or ceramic fibres obtained by electrospinning use to present high porosity and are all stuck together due to drying or calcination of the gel, therefore they form films or mats and are difficult to post-process to form different structures. Also, these porous fibres tend to be very fragile.[1]

Laser spinning is a new technique that makes continuous nanofibres in a non-woven form. This process spins fibres with diameters which vary from a few nanometer to several microns.

The method involves the use of a high-energy laser to melt small amounts of a precursor material to create a super-fine filaments that are lengthened and cooled by a powerful jet of gas. This technique allows synthesizing high quantity of ultra-long nanofibres at high speeds under ambient conditions. The versatility of the laser spinning process was also demonstrated, showing that it can be used with several precursor materials, obtaining large quantity of nanofibres with variable compositions that cannot be produced with other techniques.[19,20] Among the advantages of this technique are the high production rate, in the order of electrospining; the fibres have very long lengths and are free-standing and separated so they can be easily ordered, woven or formed into different structures adapted to different applications. Furthermore, this technique can be scalable for high production.

In this work, the laser spinning process is demonstrated to fabricate glass nanofibres containing different amounts of silver nanoparticles. Pellets of a soda-lime glass containing different content of silver nanoparticles were used as precursor. The antimicrobial activity of these silver glass fibres has been tested against Escherichia coli (Gram negative bacteria), one model biological contaminant.

Experimental procedure

Pellets of glass-nAg

Based on our early works [21, 22], homogeneously dispersed silver nanoparticles embedded into glassy matrix, with a 5 and 10 wt.% content of silver, were obtained following a simple and reliable bottom-up route: A commercial soda-lime glass with the following chemical composition (mol.%): 70.30 SiO_2, 0.92 B_2O_3, 15.34 Na_2O, 7.62 CaO, 0.03 K_2O, 4.78 MgO, 1.01 Al_2O_3, 0.01 Fe_2O_3, and the corresponding fraction of vitellinate-nAg [i.e., commercial protein with silver nanoparticles (batch nº 127, ARGENOL S.L.)] were homogeneously blended in isopropyl alcohol overnight under constant stirring. After the suspensions were dried at 60ºC for 4 h, the homogeneous mixtures were uniaxially pressed into pellets (Ø~4 cm) at 250 MPa. Next, they were sintered in air in three steps in order to ensure a complete elimination of the organic compounds from vitellinate; by heating at a rate of 3 ºC/min to 350, 500 ºC and to 725 ºC, and holding for 10, 4 and 1 h, respectively. For a comparative purpose, soda-lime glass pellets without silver nanoparticles were also obtained. In this case, they were sintered in air by heating at a rate of 10 ºC/min to 750 ºC and holding for 1 h.

Preparation of the glass nanofibres-nAg

The glassy pellets previously obtained were subsequently processed by means of laser spinning technique, the process is depicted in Figure 1. This technique entails using a high power laser to melt a small volume of the precursor material up to high temperatures. In these experiments, a CO_2 laser (wavelength of 10.6 µm) was operated in continuous wave mode emitting a power of 1.5 kW. The laser radiation was focused at 14 mm over the surface of the sample using a convergent lens with focal length of 190 mm to produce the suitable irradiance to melt the precursor. The laser has a relative movement with regard to the pellets being irradiated (constant speed of 5 mm/s), generating a quasi-stationary small volume of melted material under the laser beam. At the same time, a supersonic gas jet was injected in this volume of molten material by an off-axis de Laval nozzle (air at pressure of 10 bar). The high speed gas jet is responsible of the extremely quick elongation and cooling of this small volume of the viscous material, producing its evolution from pendant drops into long filaments. Thus high form factor fibres are formed. Also, the high cooling rate produces amorphous nanofibres. Further details on this technique are reported elsewhere.[23]

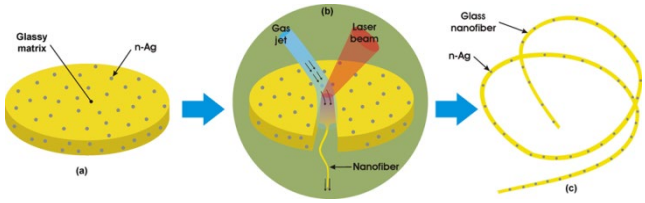

Fig. 1 Scheme depicting the process of production of the nanocomposites: the precursor material is a pellet of soda-lime glass containing silver nanoparticles (a). This pellet is processed by Laser Spinning (b) to produce the nanocomposite consisting in silver nanoparticles embedded in the glass nanofibres (c).

Characterization techniques

Infrared spectroscopy in transmission in a vacuum atmosphere with a Fourier transform infrared spectrometer (Bruker IFS 66v/s) was performed. The optical absorption spectrum was measured in the range from 200 to 800 nm using a Varian Cary 4000 UV-Vis spectrophotometer to determine the silver surface plasmon resonance. The XRD analyses of powdered samples were carried out in a Bruker D8 diffractometer using CuKα radiation working at 40 kV and 30 mA in a step-scanning mode from 4º to 70º with a step width of 0.05º and a step time of 0.5 seconds. The morphology of the glass fibres was examined by scanning electron microscopy (SEM) (Nova TM NanoSEM-FEI Company). The silver particle size and the morphological aspects were studied by Transmission Electron Microscopy (TEM) (Jeol microscope model 1011).

Antibacterial tests

The glass fibres were conformed in discs with a diameter of 1 cm by axial press in a cylindrical Y-TZP zircon dye at ~ 10 MPa. As it can be seen in the SEM micrographs of the inset of Figure 7, there are spaces between adjacent fibres, resulting in a non-uniform interconnected porous structure, which could be an important factor for some possible applications such as water or air filtering. The antibacterial activity of the glass fibres with and without silver was evaluated against *Escherichia coli W3110* (Gram negative bacteria). One face of the fibrous disc was covered with 50 µL of melted soft agar (LB containing 0.6% agar) containing approximately 10^6 CFU/mL of the bacterial inoculum. After solidification, the thickness of the agar layer was of about 1.5 mm. The discs with the agar layer were incubated at 37 ºC for 40 h in Petri dishes containing a wet filter paper to prevent agar from drying. After incubation, the agar was removed and cut into small pieces. These pieces were immersed into 1 mL of M9 minimal salts media[24] and shaken for 6 h to allow bacteria to diffuse out of the agar. The number of bacterial cells present in the minimal salts medium was determined by plating serial dilutions onto plates of solid LB media (LB containing 1.5% agar). After incubating the

plates at 37ºC overnight, the number of colony forming units was determined. Discs of silver free glass fibres were also tested. Assays were carried out in triplicate.

Results and discussion

Morphology of silver glass nanocomposite

Figure 2A shows an overall view of the macroscopic appearance of the obtained glass nanofibres, they resemble a cotton ball and have very similar consistency. Figure 2B presents a SEM image showing the typical morphology of the fibres.

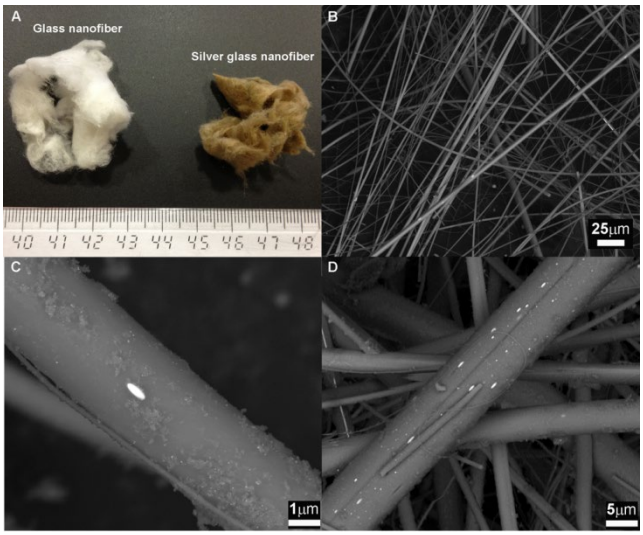

Fig. 2 A) Macroscopic image of the glass nanofibres. B) SEM micrograph of the fibres obtained with secondary electrons at low magnifications showing their morphology. C and D) SEM micrographs obtained with backscattered electrons from fibres with different content of silver: C) fibres obtained from precursor with a silver content of 5 wt.%. D) fibres obtained from precursor with a silver content of 10 wt.%.

Cross sectionally round nanofibres were obtained for all the glasses evaluated. Each fibre has a near constant diameter that is almost perfectly uniform along its whole length and is smoothly curved. The diameters of different fibres vary from tens of nanometers up to several micrometers. The fibres appear completely separated, there is no adhesion among different fibres. Also, they are dense, non porous, with high consistency and flexibility, then allowing their easy manipulation without breaking. Therefore they can be woven or formed into different structures. Some particles and debris attached on their surfaces can be also observed. The formation of these particles is related to the thermophysical properties of the liquid: the ratio of viscosity to surface tension of the viscous fluid brings about whether the elongational flow will yield a fibre, or the surface tension driven flow will provoke break-up of the fluid filament into droplets, and hence formation of particles.[20]

Silver nanoparticles are distributed throughout the fibres, SEM images obtained from backscattered electrons reveal the presence of the silver particles (Figures 6C and D). A good dispersion quality was achieved and no significant agglomeration was observed. Both silver glass fibres present some elongated silver nanoparticles; the fibre with higher content of silver shows greater quantity of these particles. They are formed due to the elongational stresses and extremely high cooling rates that molten silver glasses suffer during the formation of the fibres by laser spinning.

The size and morphology of the silver nanoparticles were studied by TEM (Figure 3). It is noteworthy that the procedure followed to obtain the nanofibres did not significantly agglomerate the silver nanoparticles. Most of the particles are spherical in shape with diameter ranging from 2 to 50 nm. In the case of the fibre glass with a 5 wt.% content of silver other shapes like hexagonal and nanorods are observed (Figure 3A). A visible example of the elongated silver particles is shown in Figure 3C. The size of the silver nanoparticles observed in the nanofibres is very similar to that reported in the precursor glass matrix (5-50 nm),[22] denoting an absence of agglomeration during the laser spinning process. This may be due to the fact that the process of nanofibre formation is very fast –in the order milliseconds– then preventing from metal diffusion through the viscous molten silicate. This outcome may be a significant advantage to produce other nanocomposites containing different metal nanoparticles embedded in a variety of inorganic glasses.

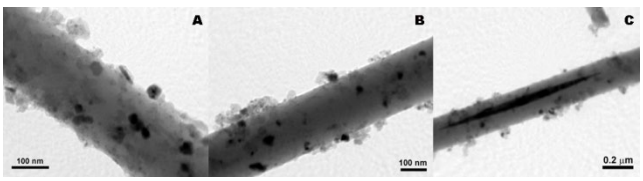

Fig. 3 TEM micrographs corresponding to: A) silver glass nanofibres (5 wt.% nAg), B) anc C) silver glass nanofibres (10 wt.% nAg).

Characterization

FTIR absorption spectral curves of glass nanofibres with and without silver are illustrated in Figure 4. For a comparative purpose the spectra of the precursor soda-lime glass is also included. The absorption bands ranging from 400 to about 1400 cm^{-1} are attributed to silicate network group vibrations with different bonding arrangements: the peak at about 470 cm^{-1} is assigned to Si-O-Si bending vibration; the peak at about 780 cm^{-1} is assigned to Si-O-Si symmetric stretching, and the peak at around 1050 cm^{-1} is assigned to Si-O-Si asymmetric stretching.[25] Bands located throughout the 1500-3700 cm^{-1} region are shown to be due to the components of the stretching modes of the bound hydroxyl groups. The bending mode of the water molecule provides at least one band around 1640 cm^{-1}. Bands in the range of 2450-3700 cm^{-1} are assigned to the asymmetric and symmetric stretching modes of interstitial H_2O molecules. The peak at around 3440 cm^{-1} is assigned to vibration of molecular water.[25, 26] There is very slight variation in the FTIR spectral curve profiles of the nanosilver containing glass nanofibres in comparison with the spectrum of the silver free glass nanofibres, only bands within the range 1539-1745 cm^{-1} have shown some slight differences (shown magnified in the inset of Figure 4). These bands are attributed to the stretching

modes of (Si)O-H in a site in which the (Si)O-H group forms the strongest hydrogen bonding with the non-bridging oxygen of a glass matrix.[26] These results show that laser spinning technique does not affect the original structure of the starting soda-lime glass.

Fig 4 Infrared spectra of the glass nanofibres. A magnified range of the spectra is shown in the inset.

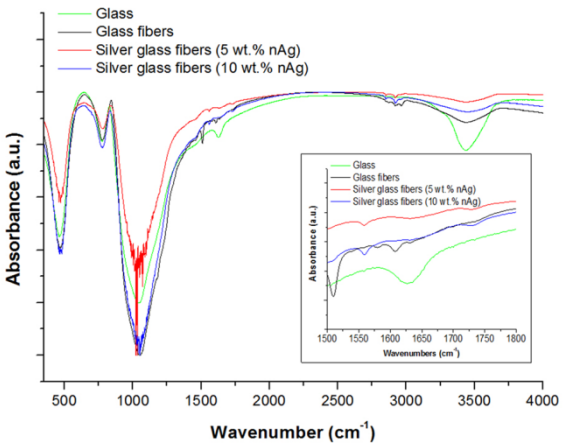

UV-Vis spectrum is quite sensitive to the formation of silver nanoparticles. Localized surface plasmon resonance of a silver nanoparticle is characterized by the absorption and scattering of incident light (together referred to as extinction) at specific resonant wavelengths. The peaks that define the extinction spectrum of a particular nanoparticle depend on a number of factors, including the size, shape, aggregation and structure, as well as the dielectric environment of the nanoparticle.[27]

Fig. 5 UV-Vis spectra of silver glass nanofibres with different content of silver nanoparticles.

The absorption spectra of the nanosilver containing glass nanofibres are shown in Figure 5. Both samples present the particular surface plasmon resonance of silver nanospheres located around 420 nm, leading to a characteristic greenish colour (see Figure 2A and inset Figure 7).

The XRD patterns of the nanosilver glass nanofibres (Figure 6) corroborate the presence of silver, the peaks can be indexed to the three strongest reflection peaks (111), (200), (220) of the face-centered cubic silver structure (JCPDS 87-0720). The XRD pattern corresponding to the silver free glass nanofibres is identical to the starting soda-lime glass one, which means no devitrification took place during the laser spinning process.

Fig 6 XRD patterns of glass nanofibres with and without silver nanoparticles.

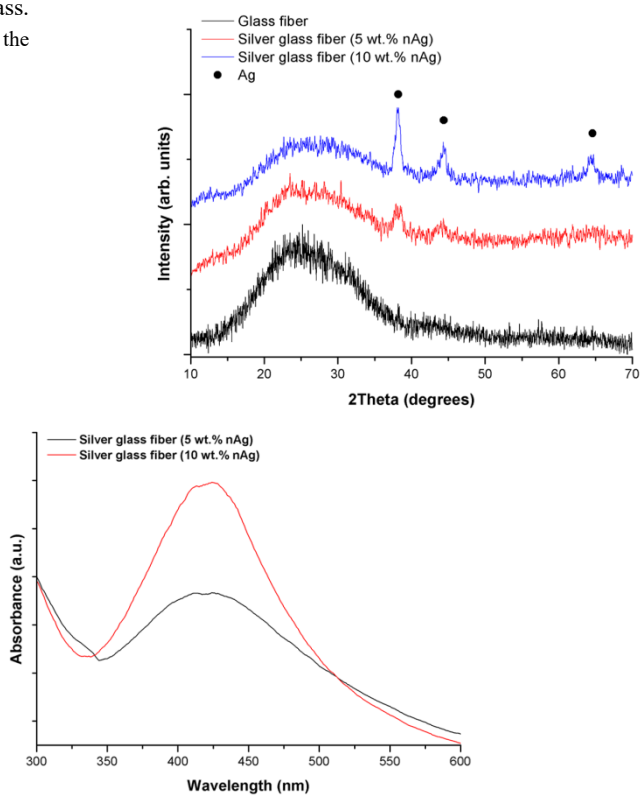

Antimicrobial Activity

The antibacterial capacities of the silver glass nanofibres against Gram negative *E. coli* were explored by a viable cell counting method. The biocidal activity of the silver glass nanofibres is expressed as the logarithm reduction in viable counts of the test bacteria (CFU mL^{-1}) according to the equation:

$$\text{Logarithm of reduction } (\log\eta) = \log A - \log B \quad (1)$$

[Eq.1]

where A is the number in viable cells in the control sample (no biocide added) and B is the number of viable cells present in the problem samples after 40 h of growth.

Silver glass nanofibres showed a very high biocide activity against the Gram negative bacteria tested (Figure 7), achieving a logarithm of reduction ca. 5, which means a highly efficient disinfection.

Fig. 7 Logarithm of reduction of glass nanofibres with and without silver after 40 h of biocide tests. Insets show pictures and SEM micrographs of the pellets of the nanosilver glass nanofibres before the biocide tests. (Diameter of the pellets: 1 cm).

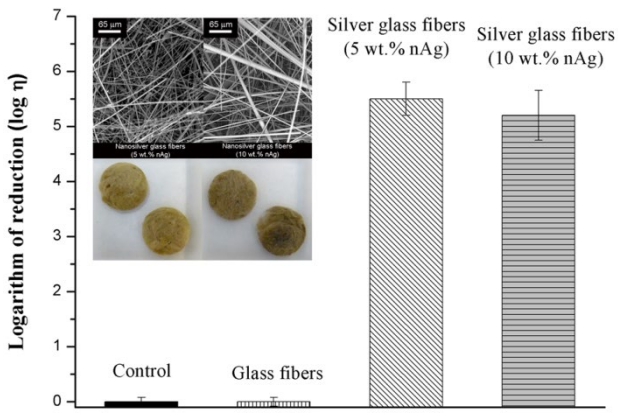

A higher content of silver nanoparticles embedded into the fibre (> 5 wt.%) did not lead to a higher activity, since both nanosilver glass fibres showed a similar biocide activity. For a comparative purpose, the test was also carried out with the glass fibres without silver. As it was expected, no biocide activity was observed for these fibres.

The main advantage that these nanofibres offer in comparison with other biocide glass fibres impregnated with silver nanoparticles,[8-10] is that in this particular case, silver nanoparticles are not only on its surface, as the decorated ones previously mentioned, but also embedded into the fibre, hence its bactericidal efficacy should have a longer-lasting effect.

To conclude, here we report a new technique for the production of nanocomposites composed of glass nanofibres with metal nanoparticles. In comparison with the previously mentioned works which all rely on the technique of electrospinning, the present technique has the advantage of producing free-standing and separated nanofibres which can be easily post-processed to form woven mats or other structures. Furthermore, it doesn't undergo the drawbacks mentioned by other authors: such as agglomeration of metal nanoparticles; low flexibility and high fragility due to the elevated porosity of the fibres and attachment of the fibres in the films produced; and limited compatibility of polymers with some metal salts, making it difficult to develop new types of spinnable sol-gel solutions. Finally, this technique can be easily extended to different metal-glass stable compositions since the very fast method of nanocomposites formation relies in a mere physical process which does not involve chemical interactions. All these novel characteristics will potentially open up a whole new range of applications.

Conclusions

In summary, laser spinning technique has been successfully used to fabricate glass nanofibres with different content of silver nanoparticles. These silver glass nanofibres displayed a significant antibacterial performance (logarithm of reduction >5). The metal nanoparticles are well-dispersed not only on the surface but also embedded into the non-woven uniform nanofibres, which leads to a long lasting durable antimicrobial effect.

The produced nanocomposites are formed with dense and flexible nano- and microfibres which are free-standing and separated, then allowing for post-processing to weave or form them into different structures depending on the applications. The metal nanoparticles conserve their chemical integrity without evidences of oxidation, contamination or significant agglomeration. The process doesn't involve any chemical interaction of the metal nanoparticles with the glass fibres, therefore it may be applied to different stable combinations of metal and glass or ceramic. Consequently, these outcomes suggest that this technique may present a potential advantage to produce nanocomposites containing different metal nanoparticles embedded in a variety of glass or ceramic nanofibres.

Acknowledgements

We are grateful to L. Yuste for excellent technical assistance. B. Cabal acknowledges financial support from JAE-Doc program (CSIC, cofounded by FSE). This work was supported by Xunta de Galicia (10DPI303014PR) and the Spanish Ministry of Science and Innovation (MICINN) under the project MAT2009-14542-C02-02.

Notes and references

[*a] *Nanomaterials and Nanotechnology Research Center (CINN-CSIC-UO-PA), Parque Tecnológico de Asturias, Llanera, 33428, Spain, Tel: +34985733644; E-mail: b.cabal@cinn.es*

[b] *Department of Applied Physics, University of Vigo, 36310, Vigo, Spain*

[c] *National Center of Biotechnology (CNB-CSIC), Cantoblanco, 28049, Madrid, Spain.*

[d] *Institute of Materials Science of Madrid (ICMM-CSIC), Cantoblanco, 28049, Madrid, Spain.*

1 Y. Dai, W. Liu, E. Formo, Y. Sun and Y. Xia, *Polym. Adv. Technol.*, 2011, **22**, 326.
2 X. Lu, C. Wang and Y. Wei, *Small*, 2009, **5**, 2349.
3 V. Thavasi, G. Singh and S. Ramakrishna, *Energy Environ. Sci.*, 2008, **1**, 205.
4 D. Li, J. T. McCann, M. Gratt and Y. Xia, *Chem. Phys. Lett.*, 2004, **394**, 387.
5 E. Formo, E. Lee, D. Campbell and Y. Xia, *Nano Lett.*, 2008, **8**, 668.
6 Y. Li, J. Gong, G. He and Y. Deng, *Mater. Chem. Phys.*, 2012, **134**, 1172.
7 M. Botes and T. E. Cloete, *Crit. Rev. Microbiol.,* 2010, **36**, 68.
8 G. Nangmenyi, W. Xao, S. Mehrabi, E. Mintz and J. Economy, *J. Water Health*, 2009, **7**, 657**.**
9 G. Nangmenyi, X. Li, S. Mehrabi, E. Mintz and J. Economy, *Mater. Lett.*, 2011, **65**, 1191.
10 G. Nangmenyi, Z. Yue, S. Mehrabi, E. Mintz and J. Economy, *Nanotechnol.***,** 2009, **20**, 495705 (10pp)
11 Q. Shi, N. Vitchuli, J. Nowak, J. M. Caldwell, F. Breidt, M. Bourham, X. Zhang and M. McCord, *Eur. Polym. J.*, 2011, **47**, 1402.
12 C. D. Saquing, J. L. Manasco and S. A. Khan, *Small*, 2009, **5**, 944.
13 B. Carlberg, L-L. Ye and J. Liu, *Small*, 2011,**7**, 3057.
14 E. Han, D. Wu, S. Qi, G. Tian, H. Niu, G. Shang, X. Yan and X Yang, *ACS Appl. Mater. Interfaces,* 2012, **4**, 2583.
15 A. C. Patel, S. Li, C. Wang, W. Zhang and Y. Wei, *Chem. Mater.,* 2007, **19,** 1231.
16 Z. Ma, H. Ji, Y. Teng, G. Dong, D. Tan, M. Guan, J. Zhou, J. Xie, J. Qiu and M. Zhang, *J. Mater. Chem.*, 2011, **21**, 9595.
17 X. Wang, H. Fan, P. Ren, H. Yu and J. Li*, Mater. Res. Bull.*, 2012, **47**, 1734.
18 Z. Ma, H, Ji, D. Tan, Y. Teng, G. Dong, J. Zhou, J. Qiu and M. Zhang, *Colloid Surfaces Physicoch. Eng. Aspects*, 2011, **387**, 57.
19 F. Quintero, J. Pou, R. Comesaña, F. Lusquiños, A. Riveiro, A. B. Mann, R. G. Hill, Z. Y. Wu and J. R. Jones, *Adv. Funct. Mater.*, 2009, **19**, 3084.
20 F. Quintero, J. Pou, F. Lusquiños and A. Riveiro, *Appl. Surf. Sci.,* 2007, **254**, 1042.
21 L. Esteban-Tejeda, F. Malpartida, A. Esteban-Cubillo, C. Pecharromán and J. S. Moya, *Nanotechnol.*, 2009, **20**, 085103 (6pp)
22 L. Esteban-Tejeda, F. Malpartida, C. Pecharromán and J. S. Moya, *Adv. Eng. Mater.*, 2010, **12**, B292.
23 F. Quintero, O. Dieste, J. Pou, F. Lusquiños and A. Riveiro, *J. Phys. D: Appl. Phys.*, 2009, **42**, 065501.
24 J. Sambrook and D. W. Russell, Molecular cloning: A laboratory manual, Cold Spring Harbor Laboratory Press, Cold Spring Harbor, NY 2001.
25 M-T. Wang, J-S. Cheng, M. Li and F. He, *Physica B*, 2011, **406**, 187**.**
26 A. M. Efimov, V. G. Pogareva and A. V. Shashkin, *J. Non-Cryst. Solids*, 2003, **332**, 93.
27 Y. Sun and Y. Xia, *Analyst,* 2003, **128,** 686.